Chapter 2

Multi-User Channel Estimation Exploiting Pulse Shaping Information

2.1 Introduction

In mobile radio communications it is important to have a good estimate of the channel relating the transmitted symbols to the received samples. This channel can be modeled as an FIR-channel. A part of the dynamics described by the channel is caused by the pulse shaping performed at the transmitter in terms of modulation and at the receiver by the receive filter. If we assume knowledge of this pulse shaping, it can be used to improve the channel estimates. Fewer parameters need to be estimated from training data which leads to an improved estimation accuracy.

For multi-user channel estimation, the number of parameters to be estimated increases linearly with the number of users (transmitters) while the number of equations is limited by the length of the training sequence. Since the method presented here is economic with respect to the number of parameters to be estimated for each user, it will improve the channel estimates in line with the parsimony principle [42]. In some cases it will also make otherwise impossible joint multi-user channel estimation possible.

A commonly used channel estimation method for GSM channels that utilizes pulse shaping information can be found in [5]. Here the received training part of the signal is correlated with the modulated training sequence. The training sequence is chosen so that the correlation approximately gives the unknown part of the channel, excluding the pulse shaping. In [3] a method for channel identification is presented that discretizes the continuous convolution between the pulse shaping function

and the ”unknown” channel impulse response. This results in a parameterization of the total channel in terms of parameters for the unknown part of the channel. The parameterization is then used in order to identify the total channel.

The channel identification method presented in this chapter also derives a parameterization of the total channel in terms of parameters for the unknown part of the channel. The approach to the modeling is however different. The method is based on approximation, using a set of pulse shaping functions sampled at different time instants. The approximation is related to an interpolation between sampled versions of the pulse shaping function with different offsets in the sampling instants, similar to the approach in [1]. The approximation used in this chapter can be scaled, and more than two sampled pulse shaping functions can be involved. It will therefore not represent interpolation in a true sense but rather a linear combination of the sampled pulse shaping functions. The modeling is illustrated for the pulse shaping function used in D-AMPS (IS-54). The method and notation here is presented for a single receiving antenna, but is generalized to multiple antennas in Chapter 3. A multi-user example utilizing multiple antennas is however presented in Section 2.4.

The method in [3] is formulated as a method for multiple antennas. A closer study reveals that it decouples spatially and is thus a purely temporal method, i.e. the channels from the mobile to the each of the antennas are estimated independently. The method in this chapter is only presented as a temporal method. In the simulation example presented in Section 2.4, multiple antennas are used, but the identification is applied to each antenna independently.

Other approaches which utilize the pulse shaping information for channel estimation can for example be found in [2], and [4]. A blind method using pulse shaping information can be found in [6].

2.2 Channel model

We here first discuss the model for the channel from one user. The generalization to multiple users can be found in Section 2.3. In continuous time, with the time index denoted by t_c, a linear communication channel with linear modulation can be modeled by a *known* linear pulse shaping filter with the impulse response $p(t_c)$, and an *unknown* linear filter with the impulse response $h(t_c)$, representing the ”physical” channel the signal

passes through. In the pulse shaping filter we can include all known time-invariant linear filtering which is performed both at the receiver and the transmitter. The unknown linear filtering performed by the physical channel and possibly by unknown filtering in the receiver and transmitter can be modeled by the unknown, time invariant channel $h(t_c)$. In the frequency domain, the impulse responses $p(t_c)$ and $h(t_c)$ can be represented by their transfer functions $P_c(s)$ and $H_c(s)$. Another possibility is to use the derivative operator, defined as $p = \frac{d}{dt}$. We can then form the operators $P_c(p)$ and $H_c(p)$, which relate the input to the output in the time domain according to

$$y(t_c) = H_c(p)P_c(p)d(t_c) + n(t_c). \tag{2.1}$$

The continuous time model can therefore be illustrated as in Figure 2.1.

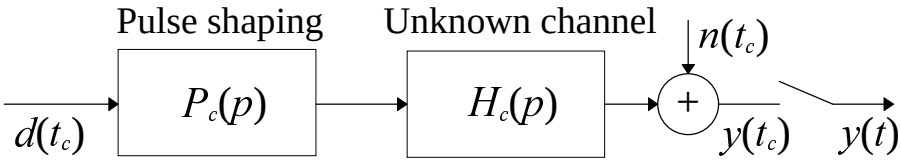

Fig. 2.1. Continuous time channel model where t_c and t denote continuous and discrete time, respectively.

The input symbols $d(t)$ are defined in discrete time t, but can be modeled as a sequence of dirac pulses, giving the continuous time signal $d(t_c)$. Also, a continuous time additive noise source $n(t_c)$ is modeled. By sampling the received signal $y(t_c)$, the discrete time output sequence $y(t)$ is obtained.

The discrete time channel from $d(t)$ to $y(t)$ can be approximated by an FIR filter, i.e.

$$B(q^{-1})=b_0+b_1q^{-1}+...+b_{nb}q^{-1} \tag{2.2}$$

were q^{-1} represents the unit delay operator: $q^{-1}d(t)=d(t\text{-}1)$. The channel model can be seen in Figure 2.2, where $n(t)$ is discrete time noise. To obtain a statistically accurate discrete time representation of the channel and the noise would require sampling of a continuous time stochastic process, see e.g. [45]. This is a rather complicated operation and for the purpose of this thesis we need not go in to further details on this issue. By using a known training sequence as input $d(t)$, the coefficients in $B(q^{-1})$ can

be estimated with a least squares method. However, we would then not utilize the information about the pulse shaping filter $p(t_c)$.

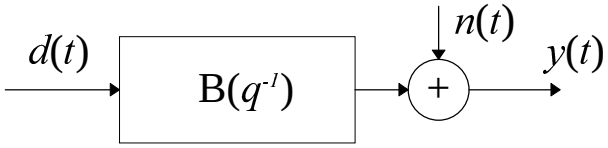

Fig. 2.2. Discrete time FIR channel model.

A first step towards incorporating the knowledge of the pulse shaping filter into the discrete time channel model is to sample $p(t_c)$ T-spaced (once per symbol interval) and form an FIR filter $P(q^{-1})$ from the so obtained samples. The discrete time model then becomes $P(q^{-1})$ followed by a T-spaced discretization, $H(q^{-1})$ of the unknown channel $h(t_c)$. We would then obtain the model presented in Figure 2.3.

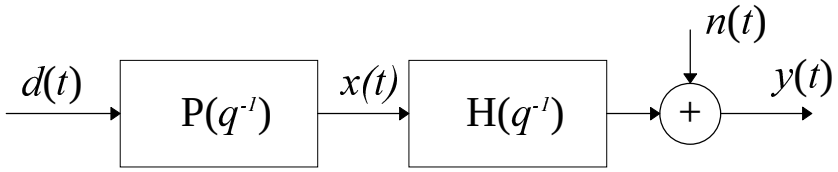

Fig. 2.3. A Discrete time channel model with a T-spaced sampled pulse shaping filter.

The estimation is now restricted to the FIR filter $H(q^{-1})$ using the ”modulated” signal $x(t)$ as the input signal. A potential problem with this method is that the model may be to crude. When designing $P(q^{-1})$ we have to choose where to sample the pulse shaping function $p(t_c)$. For a pulse passing through the physical channel and being sampled at these instants, we would have a better model than the FIR-model of Figure 2.2. A non-dispersive physical channel $h(t_c)=h_0\delta(t_c)$ would for example be represented by a channel $H(q^{-1})$ with a single unknown tap

However, for a pulse passing through the physical channel and being sampled at time instants *in-between* the chosen sampling points of $p(t_c)$, the model in Figure 2.3 will not be perfect. The received sampled pulse can then essentially be described by a linear combination of two T-spaced shifted versions of $P(q^{-1})$. Apart from a scaling, this can be viewed as an interpolation between two shifted pulse shaping filters. If we have no additional unknown channel dynamics, then the lack of perfect synchronized sampling can be accommodated by an extra tap in the channel $H(q^{-1})$. This is illustrated in the following example.

Example: Let $P(q^{-l})$ be given by

$$P(q^{-1}) = p_0 + p_1 q^{-1} + p_2 q^{-2} \tag{2.3}$$

and the unknown channel by

$$H(q^{-1}) = h_0 \tag{2.4}$$

i.e. a single-tap unknown channel. With perfectly synchronized sampling, the total channel estimate

$$\hat{B}(q^{-1}) = \hat{b}_0 + \hat{b}_1 q^{-1} + \hat{b}_2 q^{-2} = (p_0 + p_1 q^{-1} + p_2 q^{-2})\hat{h}_0 \tag{2.5}$$

will be more accurate than the traditional LS-estimate of b_0, b_1 and b_2, since only h_0 need to be estimated with the same amount of data. If, however, we have a sampling offset, we can increase the order of the unknown channel in the *model* of Figure 2.3. The channel estimate is then given by

$$\begin{aligned}\hat{B}(q^{-1}) &= (p_0 + p_1 q^{-1} + p_2 q^{-2})(\hat{h}_0 + \hat{h}_1 q^{-1}) = \\ &= p_0\hat{h}_0 + (p_0\hat{h}_1 + p_1\hat{h}_0)q^{-1} + (p_1\hat{h}_1 + p_2\hat{h}_0)q^{-2} + p_2\hat{h}_1 q^{-3}\end{aligned} \tag{2.6}$$

i.e. a linear combination of $P(q^{-l})$ and $q^{-l}P(q^{-l})$. This will give a good approximation of the total channel, since only two parameters (compared to three in the traditional case) need to be estimated, provided that the sampling offset is small.

If improved accuracy is desired in the model, more than one sampled version of the pulse shaping function $p(t_c)$ can be used, see Figure 2.4. This is similar to the approach taken in [1]. The modeling of the channel will here be divided into two branches with two different sampled versions of the pulse shaping filter, $P_{0.0}(q^{-l})$ and $P_{0.5}(q^{-l})$, with their sampling instants offset by half a symbol interval. The subscript refers to the offset of the filters center tap from the center or peak of the pulse shaping function $p(t_c)$. See, for example, Figure 2.8. The benefits of utilizing this $T/2$-spaced interpolation as compared to T-spaced interpolation will be illustrated in Section 2.4.

Each discrete time pulse shaping filter in this model is then followed by a discrete time channel, $H_1(q^{-l})$ and $H_2(q^{-l})$ respectively, see Figure 2.4.

Each pulse passing through the system will now be represented as a single tap in $H_1(q^{-1})$ and $H_2(q^{-1})$ or a combination of two or more adjacent taps. Again this can be viewed as an interpolation among adjacent sampled and shifted pulse shaping functions. Note that the interpolation is now performed among the $T/2$-spaced sampled and shifted pulse shaping functions $P_{0.0}(q^{-1})$ and $P_{0.5}(q^{-1})$. This interpolation is thus refined as compared to the T-spaced interpolation illustrated by Figure 2.3. If an even more refined model is desired, a larger number of pulse shaping filters, with less spacing between the sampling instants, can be used for the model in Figure 2.4.

In order to increase the *number of equations without increasing the number of parameters* to be estimated, fractionally spaced sampling can be utilized. Fractionally spaced sampling can be represented in the continuous time model by introducing a time advance of $T/2$ before an extra sampler as described in Figure 2.5. Note that this is, of course, not possible to realize in practice. It is used here merely to illustrate the idea of fractional sampling. If even finer sampling is desired, more branches with finer spacing can be used.

The final discrete time counterpart model, with both pulse shape interpolation and fractionally spaced sampling, is illustrated by Figure 2.6. The sampled pulse shaping functions $P_{-0.5}(q^{-1})$ and $P_{0.0}(q^{-1})$ for the "$T/2$-branch" will have their sampling instants offset by $-T/2$ from $P_{0.0}(q^{-1})$ and $P_{0.5}(q^{-1})$ in the "T-branch". It is important to note though that the same channel filters $H_1(q^{-1})$ and $H_2(q^{-1})$ can be used in the two branches.

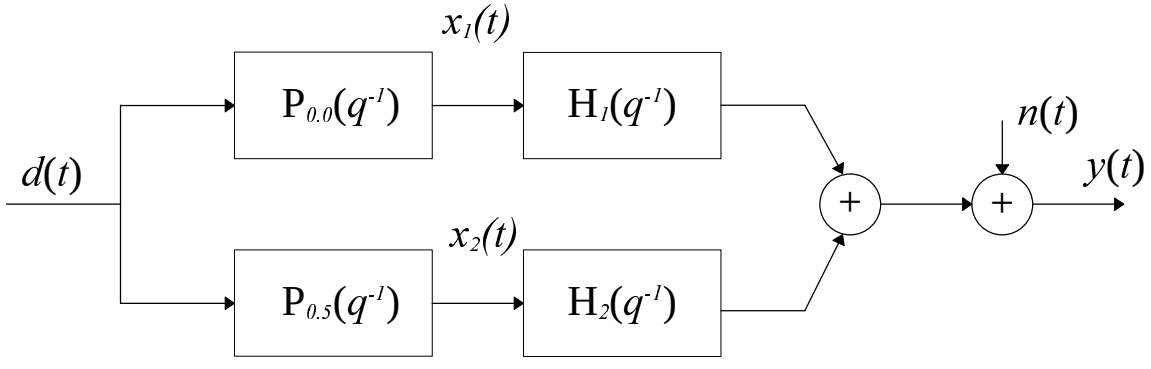

Fig. 2.4. Discrete time channel model with multiple pulse shaping filters.

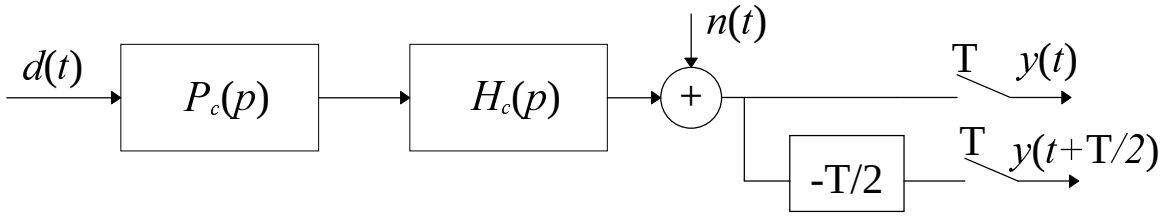

Fig. 2.5. Continuous time channel model with fractionally spaced sampling.

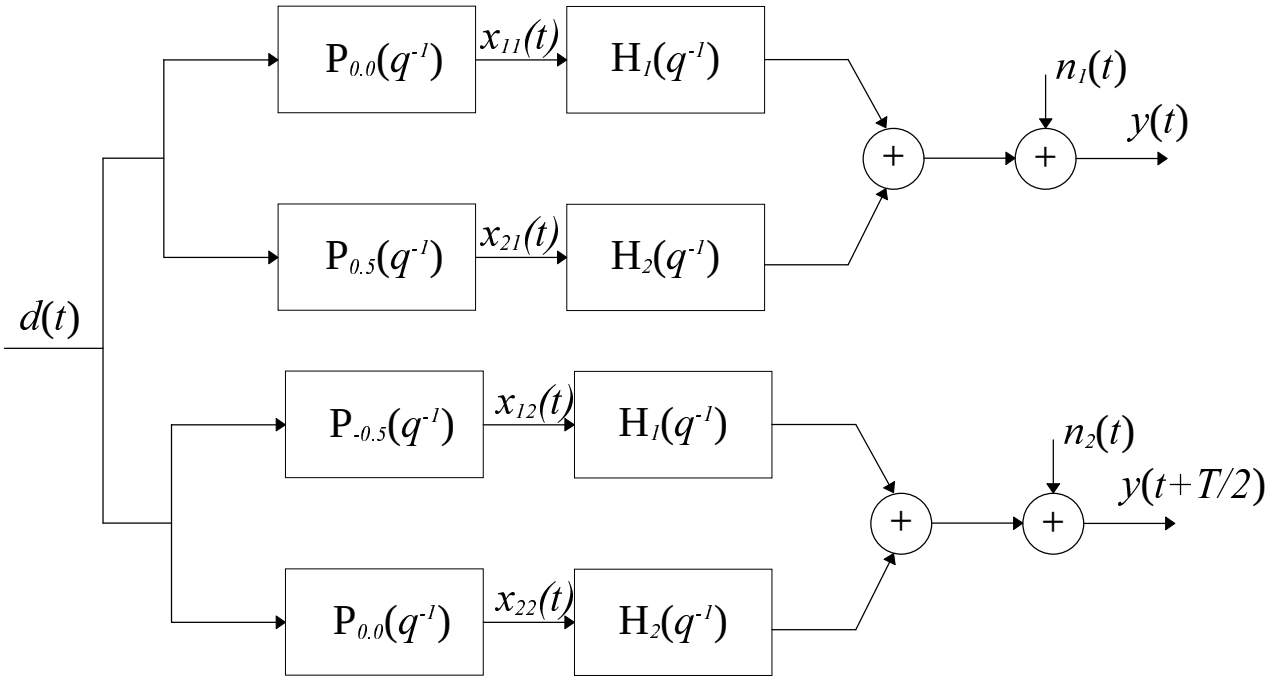

Fig. 2.6. Discrete channel model with fractionally spaced sampling and multiple pulse shaping filters per sampling branch.

The reason for this is that a good ”interpolation” in the ”*T*-branch” between $P_{0.0}(q^{-1})$ and $P_{0.5}(q^{-1})$ will also be a good interpolation between $P_{-0.5}(q^{-1})$ and $P_{0.0}(q^{-1})$ in the ”*T*/2-branch”. Thus, fractionally spaced sampling does not increase the required number of different channel submodels $H_i(q^{-1})$. An important consequence of this is that the number of parameters to be estimated in a fractionally spaced channel model does not increase while the number of equations does due to the extra data points. The estimates of the channel filters $H_1(q^{-1})$ and $H_2(q^{-1})$ can thus potentially be improved with fractionally spaced sampling. It is important to note however, that this improvement will be reduced if the fractionally spaced noise samples are temporally correlated, which will be the case for high oversampling rates (many samples per symbol) due to the limited bandwidth of the receiver filters.

2.3 Channel estimation

We shall here present the channel estimation for the case with only one user. Further more we shall use *T*/2-spaced fractional sampling and two pulse shaping filters per branch as in Figure 2.6. The equations can, however, easily be extended to arbitrary oversampling, any number of pulse shaping filters per sampling branch and arbitrary sampling instants.

The received sampled signals at time t and $t+T/2$ are collected in a row vector

$$Y(t)=[y(t)\ y(t+T/2)]. \tag{2.7}$$

Under the above assumptions, the sampled channel model can be expressed as

$$Y(t)=\mathrm{B}(q^{-1})d(t)=\mathrm{H}(q^{-1})\mathrm{P}(q^{-1})d(t) \tag{2.8}$$

with the pulse shaping matrix

$$\mathrm{P}(q^{-1})=\begin{bmatrix}\mathrm{P}_{0.0}(q^{-1}) & \mathrm{P}_{-0.5}(q^{-1})\\ \mathrm{P}_{0.5}(q^{-1}) & \mathrm{P}_{0.0}(q^{-1})\end{bmatrix} \tag{2.9}$$

and the channel vector

$$\mathrm{H}(q^{-1})=\begin{bmatrix}\mathrm{H}_1(q^{-1}) & \mathrm{H}_2(q^{-1})\end{bmatrix}. \tag{2.10}$$

We assume that $\mathrm{H}_1(q^{-1})$ and $\mathrm{H}_2(q^{-1})$ have the same order nh. By using the modulated signal

$$\mathrm{X}(t)=\begin{bmatrix}x_{11}(t) & x_{12}(t)\\ x_{21}(t) & x_{22}(t)\end{bmatrix}=\mathrm{P}(q^{-1})d(t) \tag{2.11}$$

the received signal can now be written as

$$Y(t)=\mathrm{H}(q^{-1})\mathrm{X}(t). \tag{2.12}$$

We see that we have a multiple-input multiple-output identification problem for estimating the channel $\mathrm{H}(q^{-1})$. This can, as shown below, be solved as a least squares problem.

In order to form a system of equations we vectorize equation (2.12) to obtain

$$Y(t)=HX(t) \tag{2.13}$$

where

$$H=\begin{bmatrix}h_{10} & h_{11} & \mathrm{K} & h_{1nh} & h_{20} & h_{21} & \mathrm{K} & h_{2nh}\end{bmatrix} \tag{2.14}$$

and

$$X(t) = \begin{bmatrix} x_{11}(t) & x_{11}(t-1) & \mathrm{K} & x_{11}(t-nh) & x_{21}(t) & x_{21}(t-1) & \mathrm{K} & x_{21}(t-nh) \\ x_{12}(t) & x_{12}(t-1) & \mathrm{K} & x_{12}(t-nh) & x_{22}(t) & x_{22}(t-1) & \mathrm{K} & x_{22}(t-nh) \end{bmatrix}^T \tag{2.15}$$

The unknown channel H can now be identified with the use of the least squares estimate

$$\hat{H} = \hat{R}_{YX}\hat{R}_{XX}^{-1} \tag{2.16}$$

where

$$\hat{R}_{YX} = \frac{1}{N-nb}\sum_{t=nb+1}^{N} Y(t)X^H(t) \tag{2.17}$$

and

$$\hat{R}_{XX} = \frac{1}{N-nb}\sum_{t=nb+1}^{N} X(t)X^H(t) \tag{2.18}$$

where N is the length of the training sequence, and nb+1 is the number of taps of the FIR-filter $B(q^{-1})$. The total channel $\mathrm{B}(q^{-1})$ can then be estimated by

$$\hat{\mathrm{B}}(q^{-1}) = \hat{\mathrm{H}}(q^{-1})\mathrm{P}(q^{-1}) \tag{2.19}$$

For the case with *multiple users* we can extend the channel model in Figure 2.6. This is shown below for two users. Refer to Figure 2.7 for the notation. The generalization of the channel model (2.12) is then given by

$$Y(t) = \mathrm{H}(q^{-1})\mathrm{X}(t) \tag{2.20}$$

with

$$\mathrm{H}(q^{-1}) = \begin{bmatrix} \mathrm{H}_{11}(q^{-1}) & \mathrm{H}_{12}(q^{-1}) & \mathrm{H}_{21}(q^{-1}) & \mathrm{H}_{22}(q^{-1}) \end{bmatrix} \tag{2.21}$$

and

$$\mathrm{X}(t) = \begin{bmatrix} x_{111}(t) & x_{112}(t) \\ x_{121}(t) & x_{122}(t) \\ x_{211}(t) & x_{212}(t) \\ x_{221}(t) & x_{222}(t) \end{bmatrix} = \begin{bmatrix} \mathrm{P}(q^{-1}) & 0 \\ 0 & \mathrm{P}(q^{-1}) \end{bmatrix} \begin{bmatrix} d_1(t) \\ d_2(t) \end{bmatrix} \tag{2.22}$$

The multi-user channel estimation then follows from obvious modifications of equations (2.13) to (2.19). Note that we now, with two users, have twice as many parameters to estimate but the same number of equations (output samples).

The multiple user case can be extended to include multiple antennas. The elements of $Y(t)$ in (2.7) will then be column vectors of length M, where M is the number of antennas in the array. The polynomial elements $\mathrm{H}_{ij}(q^{-1})$ of (2.21) will also be column vectors of length M. With these modifications, equations (2.20) and (2.22) will hold also in the multi-sensor case. Therefore, the channel estimation follows from obvious modifications of equations (2.13) to (2.19) in this case as well. The *single* user, multiple antenna case is treated more thoroughly in Chapter 3.

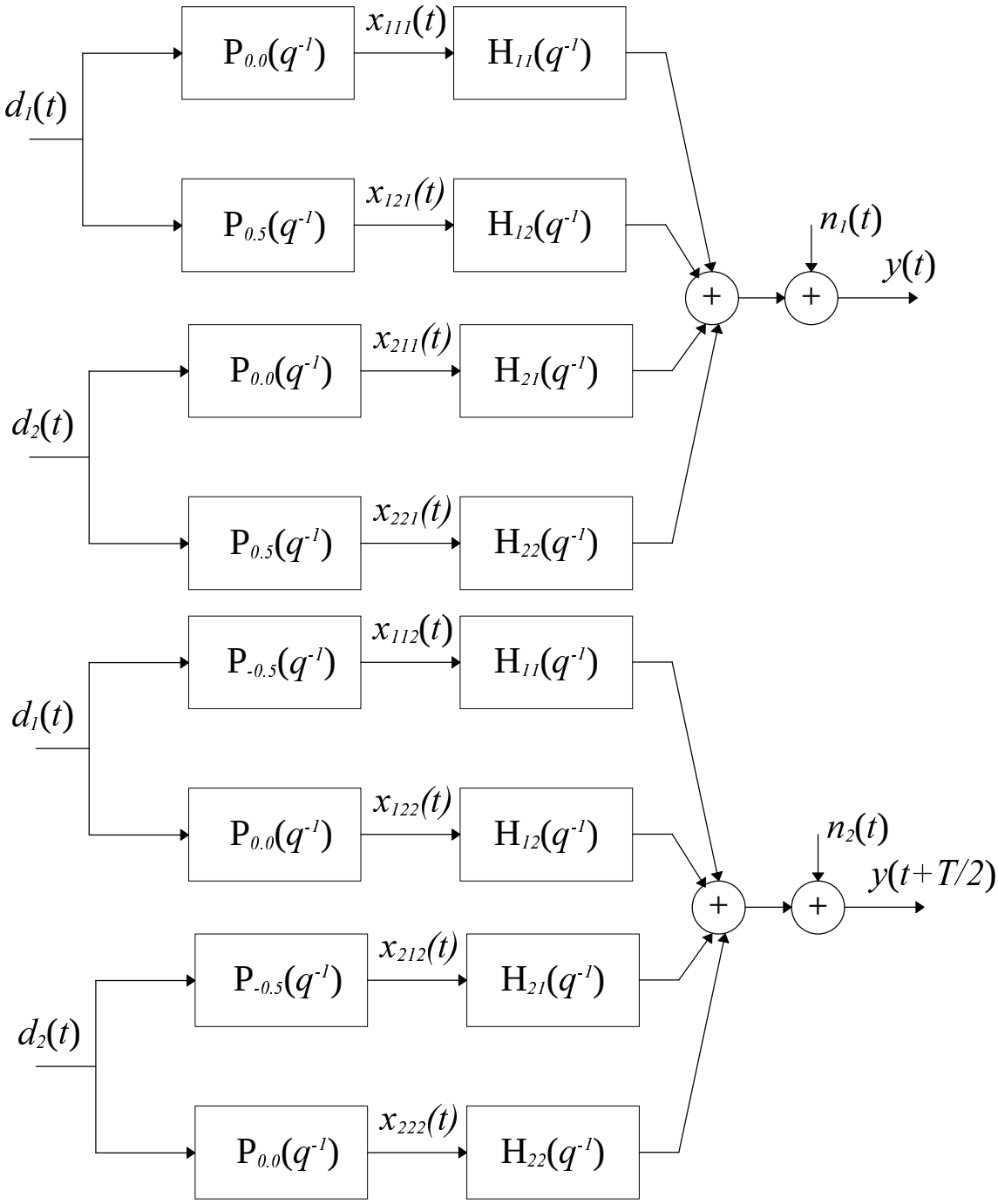

Fig. 2.7. Example of multi-user channel model for two users sending the training sequences $d_1(t)$ and $d_2(t)$ respectively.

2.4 Examples

To illustrate the pulse shaping modeling, a raised cosine pulse with a roll-off factor of 0.35 is used. This pulse form is used in the North American D-AMPS system (IS-54). In Figure 2.8, the taps of the chosen pulse shaping polynomial can be seen. The dotted line represents *T*-spaced

interpolation between time shifted versions of $P_{0.0}(q^{-1})$ and $P_{-0.5}(q^{-1})$ in the ”*T*-branch” and ”*T*/2-branch” respectively.

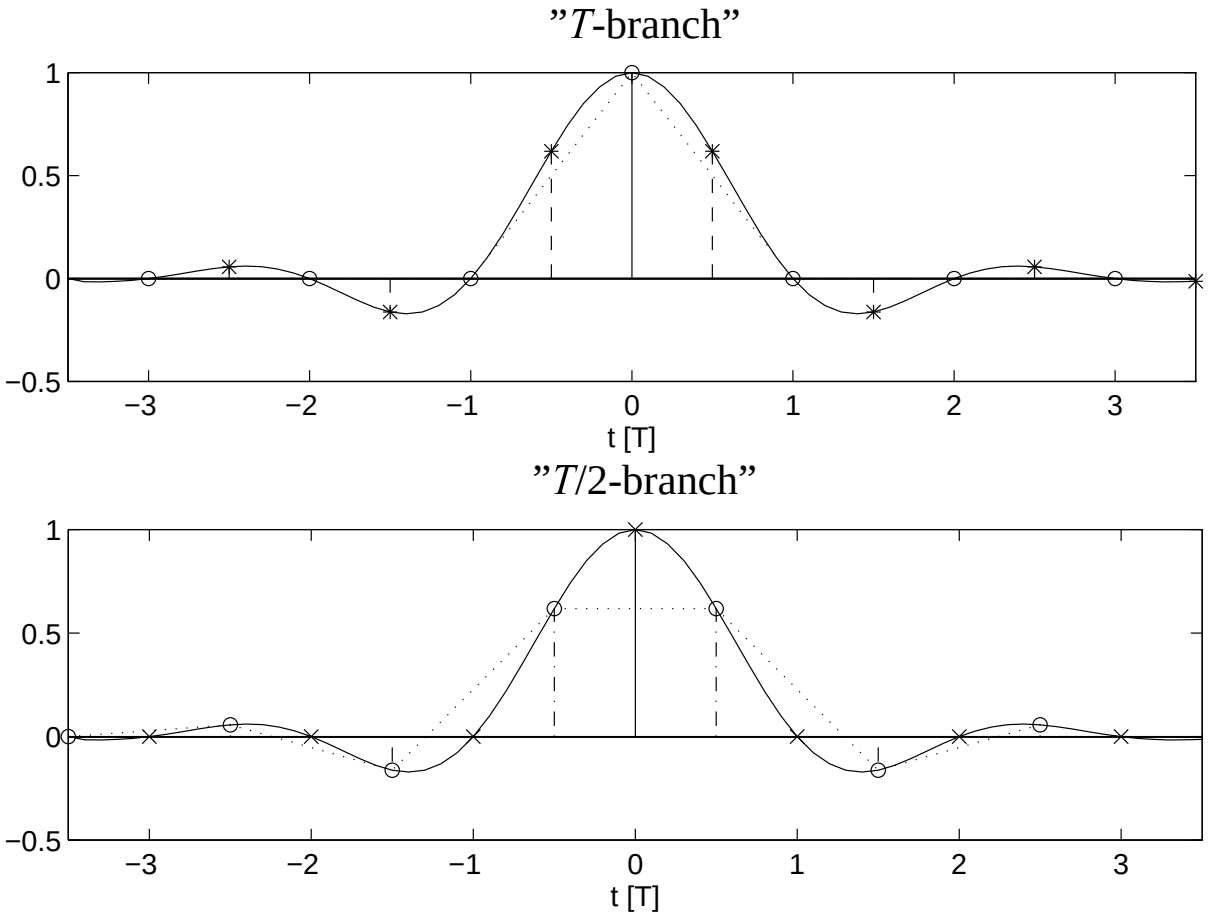

Fig. 2.8. IS-54 pulse, $p(t_c)$, and the taps of the pulse shaping filters, $P_{0.0}(q^{-1})$ (o) and $P_{0.5}(q^{-1})$ (*) for the ”*T*-branch” and $P_{-0.5}(q^{-1})$ (o) and $P_{0.0}(q^{-1})$ (x) for the ”*T*/2-branch”.

In Figure 2.9, the channel estimation error, defined in equation (2.23), for the *T*, *T*/2 and *T*/3 spaced interpolation can be seen for the noise-less case. The number of taps in the model of the pulse is chosen large enough to capture most of the energy of the pulse. A small error is however introduced because of the truncation. This can be seen in Figure 2.9 as an offset of the zero level. The error in the *T*/3 modeling is therefore smaller than that shown in Figure 2.9.

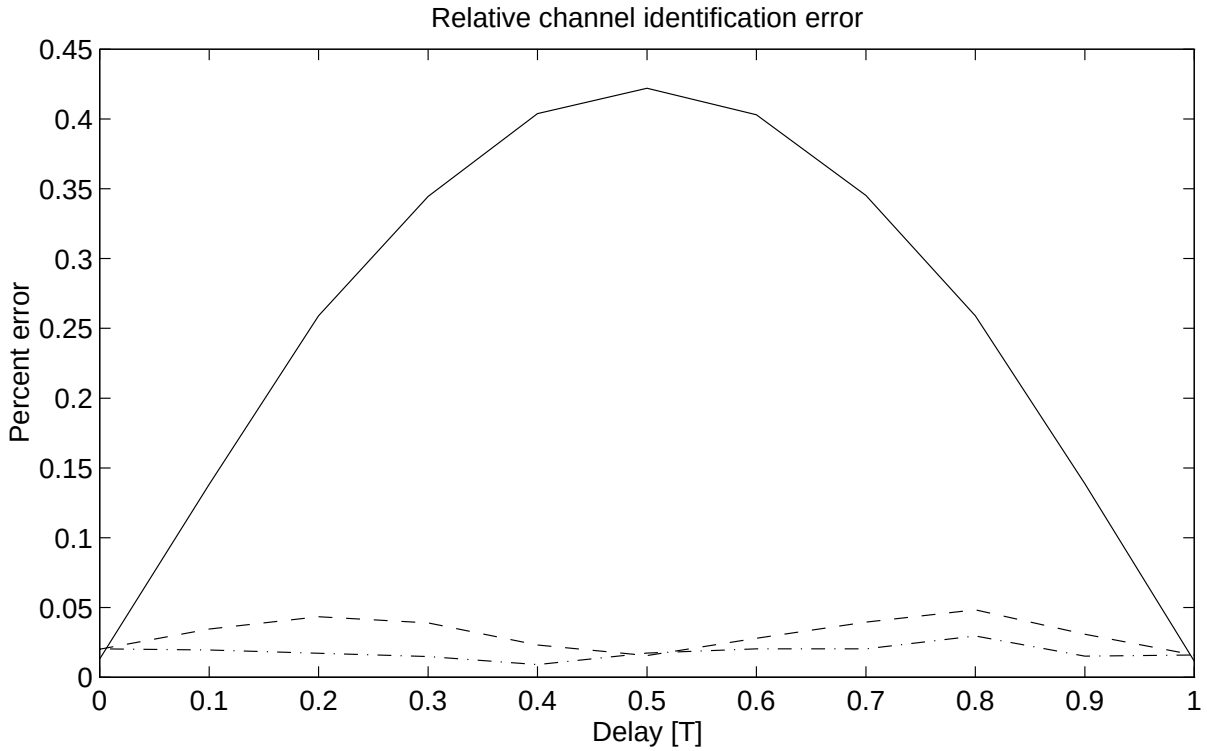

Fig. 2.9. Relative approximation error for a single IS-54 pulse with a delay between 0 and T (0.4 means a relative error of 40%). Solid: T, dashed: $T/2$ and dash-dotted: $T/3$. Note that we have an offset of the zero level because of the truncation error in the model of the pulse.

We now discuss the multi-user channel estimation example. Since it is especially advantageous to use multiple antennas for multi-user detection, we used a receiver with 4 antennas. The number of users were ranged from one to five. Each mobile had a channel with equal average power Rayleigh fading taps at delays 0.00, 0.33, 0.67 and 1.00 symbol intervals. The taps for each mobile and antenna element were fading independently. The channels were constant during each frame but independently fading between different frames. A raised cosine pulse with roll-off 0.35 was used for the pulse shaping. Other parameters were: 18 training symbols, fractionally spaced sampling (two samples per symbol), $T/2$-spaced modeling. The average SNR was 3 dB and all mobiles had equal average strength. To be able to compare the single- and multi user channel estimation methods, a single user multi channel MLSE [7] was applied to the received signal.

In Figure 2.10 the relative channel error and BER for the multi-user channel estimation example can be seen for different number of mobiles. The relative channel error is defined as

$$\left\| \hat{B} - B \right\| \Big/ \left\| B \right\| \tag{2.23}$$

using the Frobenius norm. Here $\hat{B}$ is the matrix representation (the filter taps form the columns of the matrix) of the estimated FIR-channel $\hat{B}(q^{-1})$, whereas B is the matrix representation of the true channel $B(q^{-1})$. First, not surprisingly, we can see that the joint LS channel estimation performs better than the single user LS channel estimation. Joint LS means that the channels of all known mobiles are estimated jointly, whereas one mobile at a time is modeled and estimated in the single user LS-case, while the rest of the mobiles are modeled in the noise matrix. We can also see that the method utilizing the pulse shaping information performs even better, because this method has fewer parameters to estimate per user. This becomes especially important as the number of users increases.

Note that in the multi user case, we have only considered $T/2$ spaced interpolation. It could be the case that some other interpolation, e.g. the T-spaced interpolation presented in Figure 2.3, performs even better, because the number of parameters to be estimated is further reduced.

With pulse shaping, the channel spans about 4-6 symbol intervals depending on where we choose to truncate. In the LS methods we chose to use 4 taps and in the pulse shaping method we used 2 taps in each branch of $H(q^{-1})$. The joint LS method will thus have 8 parameters *per user* to estimate with 30 equations (2 x 4 and 2 x 15 because we take two samples per symbol, have four parameters to estimate per sampling branch, and since the number of *usable* training symbols are 15). In the case of four users, we would then have more unknowns than equations.

The pulse shaping method will have 4 parameters (2 per branch) *per user* to estimate with 30 equations. As the number of users increases this difference becomes more important. We can understand this by considering a limiting case when the number of users is so many that the joint LS method has more parameters than equations while this is not the case for the pulse shaping method. In this case the joint LS method will fail while the pulse shaping method will still give some reasonable channel estimates. This is the reason why, c.f. Figure 2.10, the joint LS method degrades in performance faster with an increased number of users than the pulse shaping method does.

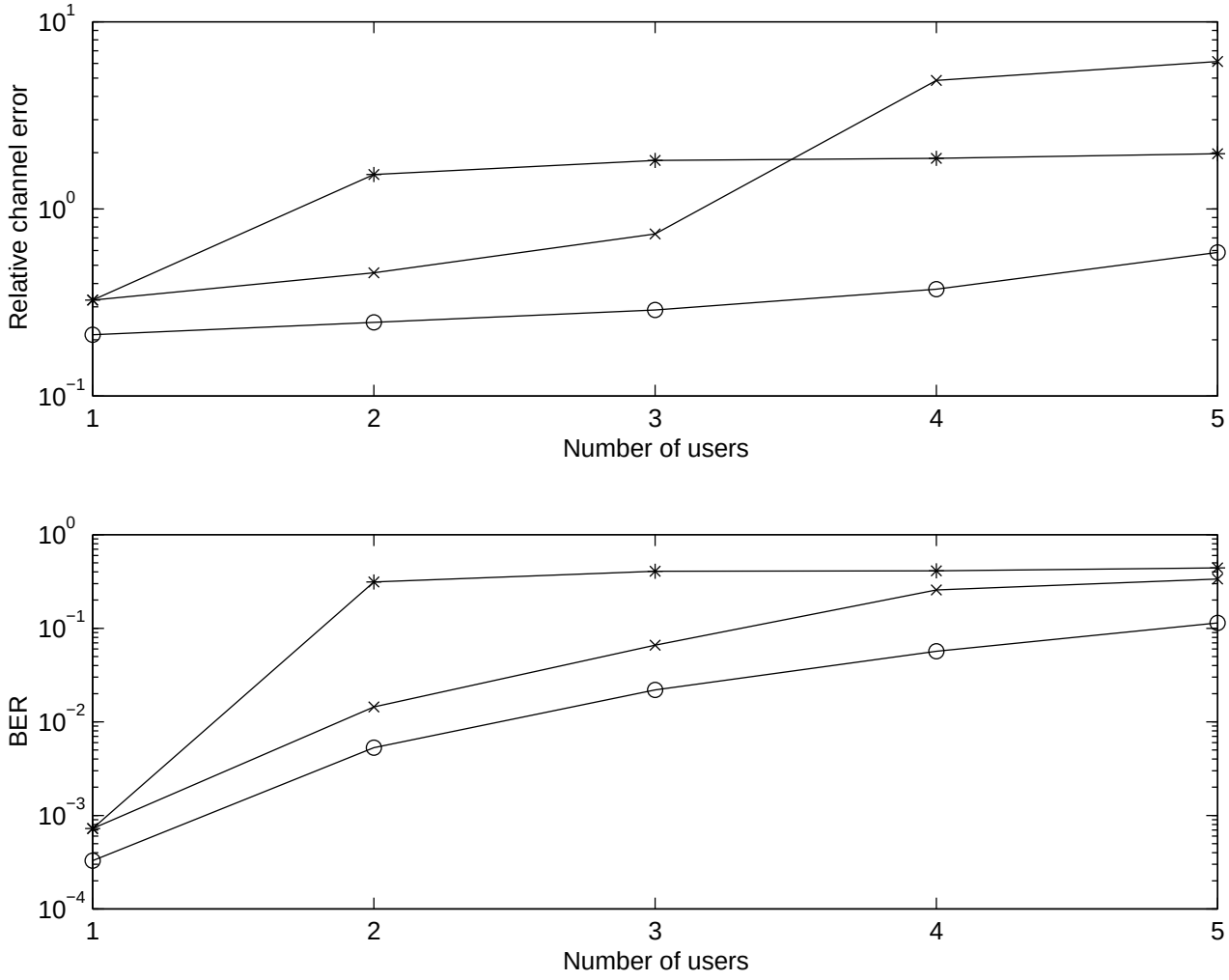

Fig. 2.10. Relative channel error and BER for the multi-user channel estimation example. Single user LS estimation (*), Joint multi-user LS (x) and Joint multi-user estimation utilizing pulse shaping information (o).